Progress In Electromagnetics Research C, Vol. 110, 167–179, 2021

A Vibration Energy Recovery Method with Application to a Semi-Active Suspension System

Yiquan Sun*, **Qingzhang Chen, Wenye Wu, and Linlin Gao**

Abstract—This paper proposes a method to recover vibration energy from a semi-active suspension system which is composed by a magneto rheological damper in parallel with a power regeneration mechanism. Central to the concept is a parity-time-symmetric (PT symmetric) circuit that is capable of providing high efficiency transmission of power and minimizing electromagnetic damping force of the power regeneration mechanism. Simulation results are presented to demonstrate the electromagnetic damping force of the power regeneration mechanism having little impact on suspension system and verify the possibility of energy recovery. The proposed control strategy pays close attention to inertial force of the power regeneration mechanism which produces indicator diagram hysteresis. To evaluate the performance brought about by the proposed method, the semi-active suspension utilizing the PT symmetric circuit is compared to the load resistance circuit. And the semi-active suspension system is implemented on a quarter car test bench to demonstrate its feasibility on a typical sine road surface.

1. INTRODUCTION

In a typical suspension system, energy from external excitations mainly is caused by the road surface and usually absorbed by its damper. This energy is converted into heat energy within the damper fluid and dissipates to the surrounding [1]. To overcome this, energy regeneration concept has been introduced to supply additional power for suspension system by harvesting energy from road surface excitation [2].

The energy harvester of suspension system wants to absorb as much energy as possible from road surface excitations and store it as a power source. Montazeri and Soleymani [3] have conducted another research on energy harvesting electromagnetic suspension. They investigated the idea of the energy regeneration in active suspension unit in hybrid electric vehicles. Martins et al. [4] proposed a combination of active and passive electromagnetic suspension systems for vehicle. A pure passive electromagnetic suspension system has been designed by Paz [5]. In the research, linear generator was designed to be implemented on the vehicle suspension system to generate energy due to road disturbance. Okada and Harada [6] proposed linear motor which provided not only better driving quality but generated electrical energy from vehicle body vibration. The vibration energy is converted into electrical energy by means of magnetic induction. Nakano et al. [7] proposed an active suspension using a DC linear motor which would be switched to regeneration mode where the actuator regenerated energy from vibration and delivers to the condenser.

Active suspension system has been developing since 1930s [8]. It consists of an actuator to produce force in the suspension system to control the motion of the car body and relative velocity between wheel and car body. It has been implemented into passenger cars. However, the high cost and large power consumption restrict its wide use. So, semi-active suspension system for vehicles has been developed fast in recent years [9]. It verifies that the performance comparable to active suspension system can be

Received 8 January 2021, Accepted 15 February 2021, Scheduled 24 February 2021
* Corresponding author: Yiquan Sun (stone@cslg.edu.cn).
The authors are with the School of Automotive Engineering, Changshu Institute of Technology, Suzhou 215500, China.

achieved by the use of a semi-active suspension system. A semi-active suspension system consists of a controllable damper that offers variable damping force and requires lower power than active suspension. A semi-active suspension system's variable damping is achieved by varying resistant to fluid flow in the damper by controlling smart fluids (electrorheological or magnetorheological fluids) [1]. It has been well considered that semi-active suspension system combines the advantages of both active and passive suspension systems [10]. Nonetheless, semi-active suspension cannot recover energy itself and requires the use of external power to start its system.

So in this paper, the idea of a semi-active suspension system in parallel with a power generation mechanism is presented. It can be used in electric intelligent driving vehicles, improves ride comfort, and increases mileage. Therefore, electric driverless tractors of intelligent agriculture will be an appropriate application. Vibration energy is stored in batteries at any time. And the platform is smooth enough for other agricultural equipment on board.

2. REGENERATIVE SEMI-ACTIVE SUSPENSION SYSTEM MODELING

A regenerative semi-active suspension system model is built to analyze its feasibility. And the designed model should have the characteristic of failure-safety [11].

2.1. A Quarter-Car Model

A quarter-car regenerative semi-active suspension system which installs a magneto rheological damper in parallel with a power regeneration mechanism is modeled as a two-degree-of-freedom dynamic system, when its vertical vibration primarily [12] is considered, and shown in Fig. 1.

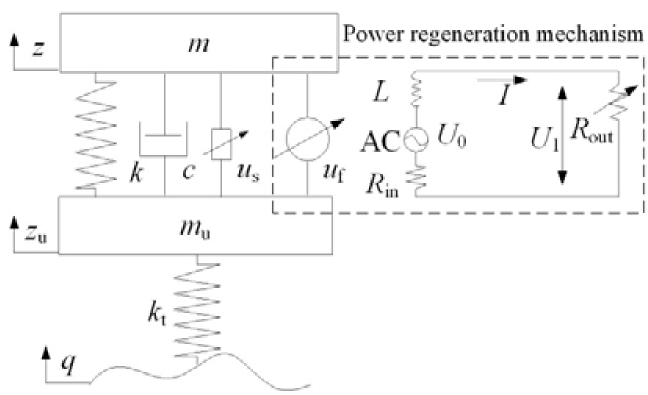

Figure 1. Quarter-car regenerative semi-active suspension model.

The dynamics of the suspension system are given by [13]:

$$\begin{cases} m\ddot{z} + c(\dot{z} - \dot{z}_u) + k(z - z_u) - u_s - u_f = 0 \\ m_u\ddot{z}_u + c(\dot{z}_u - \dot{z}) + k(z_u - z) + k_t(z_u - q) + u_s - u_f = 0 \end{cases} \tag{1}$$

where z and z_u are the absolute static displacement of the sprung mass and wheel spring; q is the road profile; m is the mass of equivalent quarter car body; m_u is the mass of wheel; k is the physical spring coefficient; k_t is the tire spring coefficient; c is the physical permanent friction coefficient; u_s is the variable controllable force provided by magneto rheological damper; u_f is the equivalent force provided by the power regeneration mechanism.

U_0 is the generated voltage by electric rotating machinery of the power regeneration mechanism, and its resistance is R_{in}; R_{out} is the resistance of load; AC is alternating current generated by electric rotating machinery. The designed model which is shown in Fig. 1 can regenerate energy all the time when suspension system is running. In this paper, we not only concern the vibration energy recovery, but also focus on the proper damping force of the suspension system.

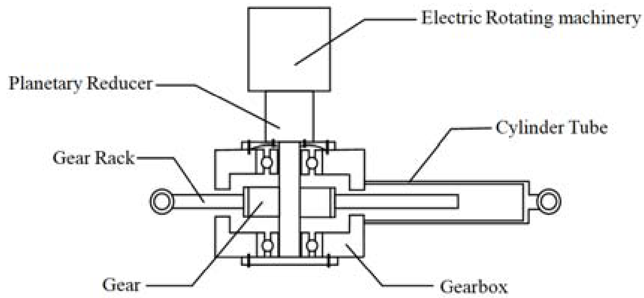

Figure 2. Power generation physical construction.

2.2. Feasibility Analysis of the Vibration Energy Recovery

The entire power generation physical construction consists of the electric rotating machinery with the gearbox, gear rack, planetary reducer, and gear, shown in Fig. 2. The generated voltage by electric rotating machinery can be written as [14]:

$$U_\text{o} = \frac{3K_\text{e}iv}{100\pi R_\text{g}} \tag{2}$$

where K_e is the EMF coefficient; v is the relative speed of suspension system; i is the gear ratio of planetary reducer; R_g is the indexing circle radius of gear. The electrical power generated by electric rotating machinery can be written as:

$$P_\text{e} = \frac{\left(U_0/\sqrt{2}\right)^2}{R_\text{in} + R_\text{out}} \tag{3}$$

The electrical power is obtained by substituting Eq. (2) into Eq. (3) which is a function of the relative speed of the system as follows:

$$P_\text{e} = 4.5 \times 10^{-4} \frac{K_\text{e}^2 i^2 v^2}{\pi^2 R_\text{g}^2 (R_\text{in} + R_\text{out})} \tag{4}$$

The electrical power varies along with suspension system's state (i.e., $P_\text{e} \propto v^2/R_\text{out}$), when other parameters are invariableness in Eq. (4). So it is possible to recover vibration energy if the load resistance and relative speed of the system have appropriate values. The electrical power will be maximum while the load resistance tends to zero. However, this will bring the maximum electromagnetic damping force as well, due to Eq. (5) which is described as:

$$f_\text{e} = 4.5 \times 10^{-4} \frac{K_\text{e}^2 i^2 v}{\pi^2 R_\text{g}^2 (R_\text{in} + R_\text{out})} \tag{5}$$

The primary parameter values of power generation physical construction are tabulated in Table 1.

Table 1. Power generation physical construction parameter values.

Parameter	**Value**
Gear ratio of planetary reducer i	16
EMF coefficient K_e	57 V/rpm
Indexing circle radius of gear R_g	0.0285 m

We can get $U_0 = 15.2\,\text{V}$ or $U_0 = 91.2\,\text{V}$ from Eq. (5) when $v = 0.05\,\text{m/s}$ and $v = 0.3\,\text{m/s}$, respectively. To prove the correctness of calculation results, the experimental setup is shown in Fig. 3.

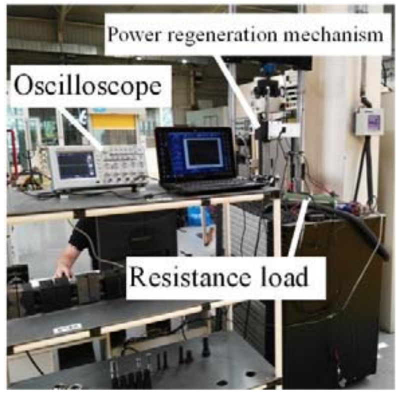

Figure 3. Power generation test bench.

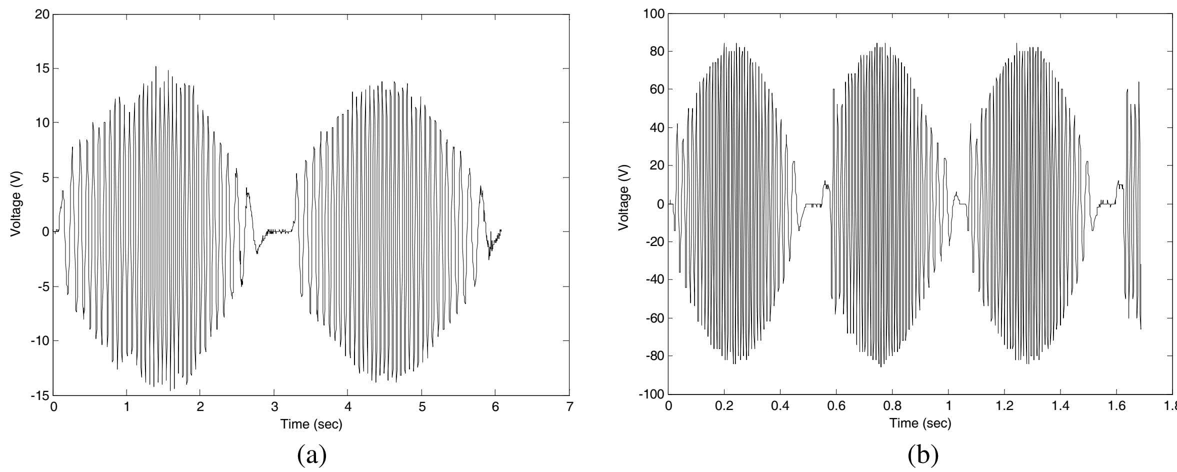

Figure 4. Output voltage with different excitation. (a) $v = 0.05\,\mathrm{m/s}$. (b) $v = 0.3\,\mathrm{m/s}$.

The simulation results are shown in Fig. 4. The peak values are close to the calculation results. So it is possible to recover vibration energy from the suspension system using power regeneration mechanism.

3. PARITY-TIME-SYMMETRIC CIRCUIT DESIGN

PT symmetric circuit changes transfer mode of power which is produced by the electric rotating machinery. The circuit can rectify current for super capacitance storage and solve the unmanageable problem of the suspension system's electromagnetic damping.

PT symmetric system is invariant under the joint parity and time reversal operation [15]. Recently, the concept of PT symmetry has been extensively explored in laser structures [16]. In this paper, we design a circuit consisting of a source resonator and a receiver resonator based on PT symmetry, as shown in Fig. 5.

The source resonator has a resonant frequency ω_1 and an overall gain rate g_1. The receiver resonator has a resonant frequency $\omega_2 \approx \omega_1$ and a loss rate γ_2. The two resonators are coupled together with a coupling rate k, which is a function of the source-to-receiver separation distance. Power is fed into the source through its gain element. The system dynamics are described as [17]:

$$\frac{\partial}{\partial t}\begin{bmatrix} \mathbf{a}_1 \\ \mathbf{a}_2 \end{bmatrix} = \begin{bmatrix} \mathrm{i}\omega_1 + g_1 & -\mathrm{i}k \\ -\mathrm{i}k & \mathrm{i}\omega_2 - \gamma_2 \end{bmatrix} \begin{bmatrix} \mathbf{a}_1 \\ \mathbf{a}_2 \end{bmatrix} \tag{6}$$

where $|a_1|^2$ and $|a_2|^2$ represent the energies stored in source and receiver resonator, respectively. In

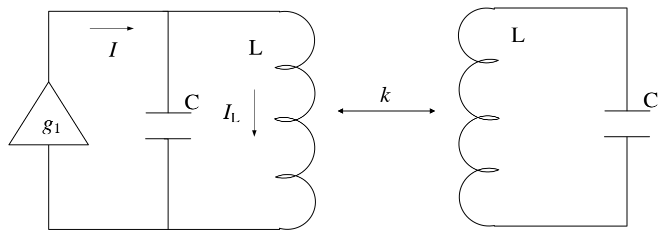

Figure 5. Couple model of source and receiver resonators.

order to find the eigenfrequencies, we let $a_1 \propto \mathrm{e}^{\mathrm{i}\omega t}$, $a_2 \propto \mathrm{e}^{\mathrm{i}\omega t}$ and then obtain the characteristic:

$$(\mathrm{i}(\omega_1 - \omega) + g_1)(\mathrm{i}(\omega_2 - \omega) - \gamma_2) + k^2 = 0 \tag{7}$$

Taking ω to be real, the real and imaginary parts of Eq. (7) are separated and obtained as:

$$(\omega - \omega_1)(\omega - \omega_2)^2 + \gamma_2^2(\omega - \omega_1) - k^2(\omega - \omega_2) = 0 \tag{8}$$

$$g_{1,\mathrm{sat}} = \gamma_2 \frac{\omega - \omega_1}{\omega - \omega_2} \tag{9}$$

where ω is the eigenfrequencies for a given loss rate γ_2 and coupling rate k. Then Eq. (9) provides the corresponding saturated gain value (i.e., $g_{1,\mathrm{sat}}$).

In the case of a matched resonance ($\omega_1 = \omega_2 = \omega_0$), Eq. (7) has the solution $\omega = \omega_0 \pm \sqrt{k^2 - \gamma_2^2}$ which supports two modes when it is in the strong coupling region ($k \geq \gamma_2$). These two modes have the same saturated gain, exactly balancing out the loss, that is, $g_{1,\mathrm{sat}} = \gamma_2$. In addition, these two modes have equal amplitude distribution, that is, $|a_2/a_1| = 1$. Therefore, it satisfies an exact PT symmetry. So this circuit is called PT symmetric circuit.

In the case of current resonance, the power transmits between source and receiver resonator. The capacity's electric field energy will convert to magnetic field energy, and the inductance's magnetic field energy will covert to electric field energy. So the power is radiated through electromagnetic wave. The LC parallel circuit of Fig. 3 has energy loss which is equivalent to resistance R. The admittance can be written as:

$$Y = \mathrm{j}\omega C + \frac{1}{R + \mathrm{j}\omega L} = \frac{R}{R^2 + (\omega L)^2} + \mathrm{j}\left[\omega C - \frac{\omega L}{R^2 + (\omega L)^2}\right] \tag{10}$$

We let imaginary part of Eq. (10) take zero, so the resonance angular frequency is:

$$\omega_0 = \frac{1}{\sqrt{1 + \left(\frac{R}{\omega_0 L}\right)^2}} \cdot \frac{1}{\sqrt{LC}} = \frac{1}{\sqrt{1 + \frac{1}{Q^2}} \cdot \sqrt{LC}} \tag{11}$$

where Q is the intrinsic quality factor (i.e., $Q = \frac{\omega_0 L}{R}$). When $Q \gg 1$, Eq. (11) can be rewritten as:

$$\omega_0 \approx \frac{1}{\sqrt{LC}} \tag{12}$$

So the resonance frequency is written as

$$f_0 \approx \frac{1}{2\pi\sqrt{LC}} \tag{13}$$

And the LC parallel circuit of Fig. 5 assumes pure resistance at the state of resonance which can be written as:

$$Z_0 = \frac{R^2 + (\omega_0 L)^2}{R} \approx Q^2 \cdot R \tag{14}$$

On the basis of Eqs. (12), (13), (14), the inductor's resistance can be written as:

$$X_L = Z_0/Q \approx Q \cdot R \tag{15}$$

And its power can be written as:

$$P_L = L \cdot I_L^2/2 \cdot \tau \tag{16}$$

where τ is the inductor's charging time (i.e., $\tau = \pi \cdot \sqrt{L \cdot C}$).

According to Eqs. (2) and (15), Eq. (16) can be rewritten as:

$$P_L = 4.5 \times 10^{-4} \frac{K_{\rm e}^2 i^2 v}{\pi^2 R_{\rm g}^2 Q^2 R} \cdot \frac{vQ}{2\pi} \tag{17}$$

According to Eqs. (5) and (14), the electromagnetic damping force can be written as:

$$f_e = 4.5 \times 10^{-4} \frac{K_{\rm e}^2 i^2 v}{\pi^2 R_{\rm g}^2 Q^2 R} \tag{18}$$

According to Eqs. (17) and (18), the value of inductor power is greater than electromagnetic damping force at the condition of $v \cdot Q \gg 2\pi$. So it is possible to recover energy from suspension system and reduce the impacts from electromagnetic damping force to suspension system controllability. To verify feasibility of the designed PT symmetric circuit, an experiment is done. The relative speed of suspension system is configured within $[-0.3\ 0.3]$ m/s which is defined as a cycle. Besides, we set $Q = 300$ and $R = 0.1\,\Omega$. The suspension system's running state is shown in Fig. 6. The electromagnetic damping force is below 2N, and the maximum regenerative power is about 22.3 W. The following test gives a deep analysis of the electromagnetic damping force effect on the indicator diagram which is shown in Fig. 7. The closed-loop area of the indicator diagram is the smallest when resistance load is the PT symmetric circuit. Therefore, it gives an ideal method to reduce impacts of electromagnetic damping force on the semi-active suspension system.

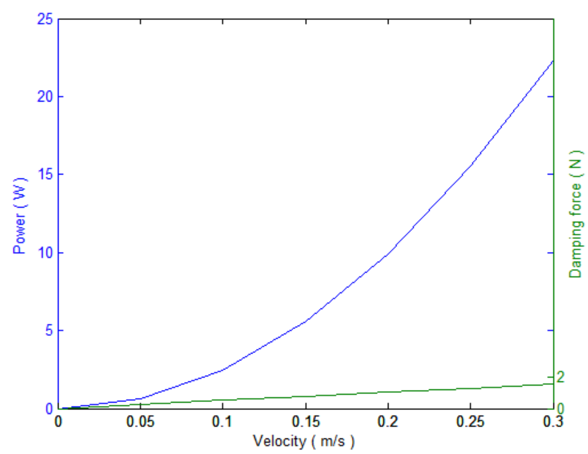

Figure 6. Regenerative power and electromagnetic damping force.

The AC power is rectified to DC power before flowing into PT Symmetric circuit. The experimental setup is shown in Fig. 8. The pk-pk voltage values of receiver resonator are close to the input DC source. PT symmetric circuit cannot transmit power when the voltage of input DC source is a subset of $\{x | -2\,\text{V} < x < 2\,\text{V}\}$ as shown in Fig. 9.

4. CONTROL STRATEGY

One of the main challenges in controllable suspension is to choose the most suitable control strategy for the system. The behavior of continuous variable damper is governed by variable viscosity smart fluids which inherit nonlinearity aspects into dampers properties [18]. As we know that skyhook control has been proven to improve the ride characteristics by reducing body acceleration [19]. And adaptive control is feed-forward and feedback where the vehicle state is fed into the controller to calculate the suitable

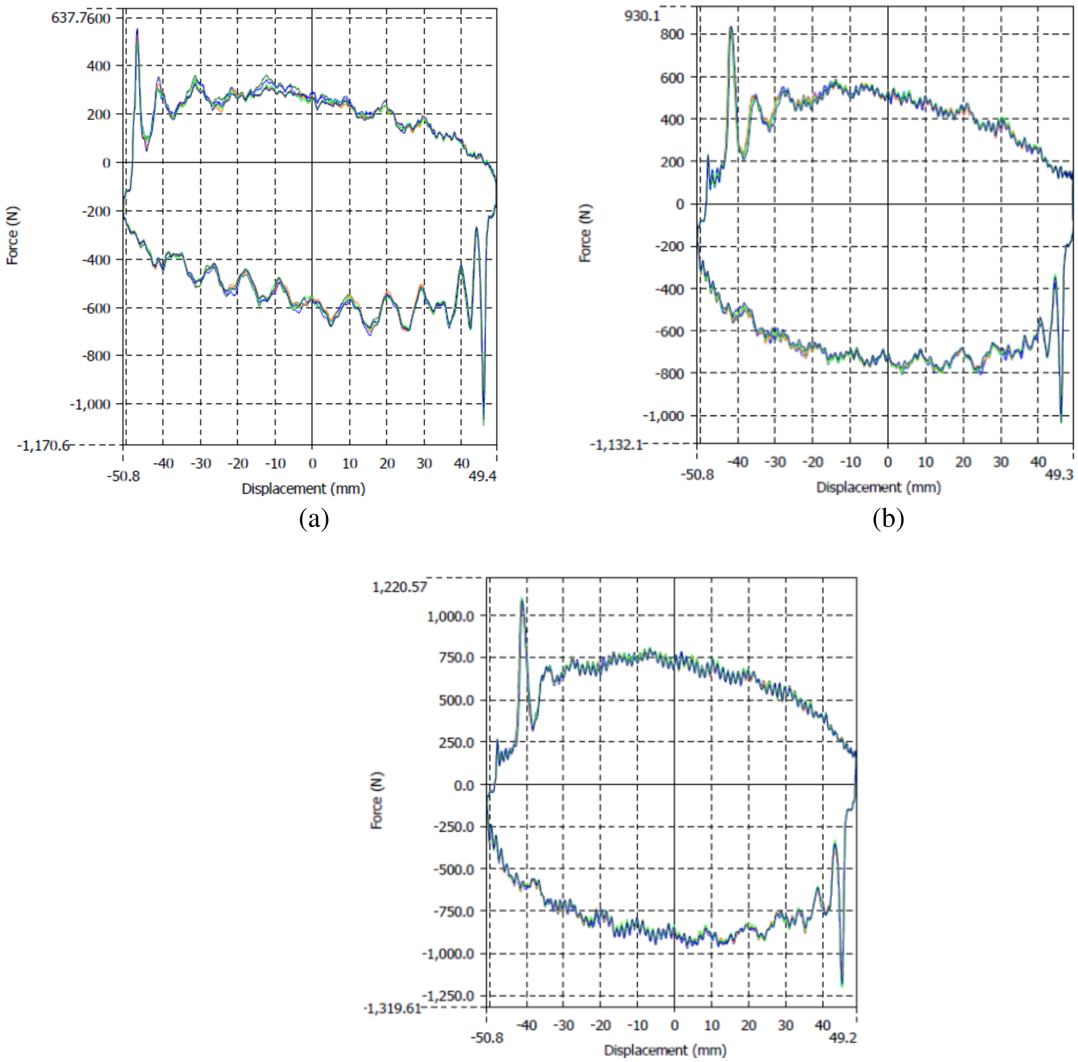

(a) (b)

(c)

Figure 7. Indicator diagram of the designed power generation physical construction. (a) Resistance load is the PT symmetric circuit. (b) Resistance load is $50\,\Omega$. (c) Resistance load is $25\,\Omega$.

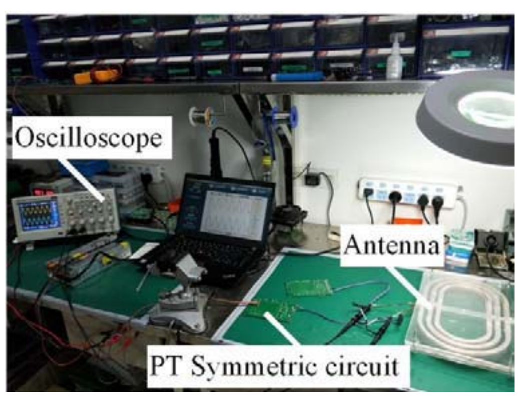

Figure 8. Experiment bench of PT symmetric circuit.

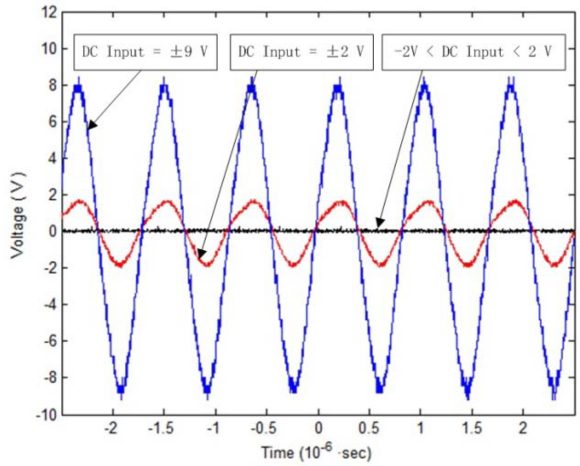

Figure 9. Voltage curve of receiver with different values of DC source input.

response. However, they are not suitable for the control of regenerative semi-active suspension [20]. The reason is that it is complicated. The damping force u_{f} consists of electromagnetic damping force f_{e}, mechanical frictional damping force produced by component friction of the power regeneration mechanism, and inertial force [21]. Because the electromagnetic damping force is under control when using PT symmetric circuit for transmitting power, the inertial force is the key to suspension's controllability. The rotary inertia of electric manufacturing, planetary reduction box, and gear will bring angular moment which hinders acceleration or deceleration of the power regeneration mechanism. The angular moment is translated into straight line inertia force by a mechanism of gear-rack. And the inertial mass can be written as:

$$m_{\mathrm{i}} = \frac{\left(i^2 J_{\mathrm{m}} + i^2 J_{\mathrm{r}} + J_{\mathrm{p}}\right)}{R_{\mathrm{g}}^2} \tag{19}$$

where J_{m}, J_{r}, J_{p} are the rotary inertia of electric rotating machinery, planetary reduction box, and gear, respectively. Therefore, the straight line inertia force can be written as:

$$f_{\mathrm{i}} = m_{\mathrm{i}}(\ddot{z}_{\mathrm{u}} - \ddot{z}) \tag{20}$$

The physical permanent friction coefficient of the power regeneration mechanism has been included in c of Eq. (1). Ignoring the impact of electromagnetic damping force, Eq. (1) can be rewritten as:

$$\begin{cases} (m + m_{\mathrm{i}})\ddot{z} - m_{\mathrm{i}}\ddot{z}_{\mathrm{u}} + c(\dot{z} - \dot{z}_{\mathrm{u}}) + k(z - z_{\mathrm{u}}) - u_{\mathrm{s}} = 0 \\ m_{\mathrm{i}}\ddot{z} + (m_{\mathrm{u}} - m_{\mathrm{i}})\ddot{z}_{\mathrm{u}} + c(\dot{z}_{\mathrm{u}} - \dot{z}) + k(z_{\mathrm{u}} - z) + k_{\mathrm{t}}(z_{\mathrm{u}} - q) + u_{\mathrm{s}} = 0 \end{cases} \tag{21}$$

To establish the suspension system's state equation, the model in Eq. (21) can be written as:

$$\begin{cases} \dot{x}_1 = \dot{z} - \dot{z}_{\mathrm{u}} = x_2 - x_4 \\ \dot{x}_2 = \ddot{z} = \dfrac{2km_{\mathrm{i}} - km_{\mathrm{u}}}{mm_{\mathrm{u}} - mm_{\mathrm{i}} + m_{\mathrm{i}}m_{\mathrm{u}}}x_1 + \dfrac{2cm_{\mathrm{i}} - cm_{\mathrm{u}}}{mm_{\mathrm{u}} - mm_{\mathrm{i}} + m_{\mathrm{i}}m_{\mathrm{u}}}x_2 - \dfrac{k_{\mathrm{t}}m_{\mathrm{i}}}{mm_{\mathrm{u}} - mm_{\mathrm{i}} + m_{\mathrm{i}}m_{\mathrm{u}}}x_3 \\ \qquad - \dfrac{2cm_{\mathrm{i}} - cm_{\mathrm{u}}}{mm_{\mathrm{u}} - mm_{\mathrm{i}} + m_{\mathrm{i}}m_{\mathrm{u}}}x_4 + \dfrac{m_{\mathrm{u}} - 2m_{\mathrm{i}}}{(m + m_{\mathrm{i}})(m_{\mathrm{u}} - m_{\mathrm{i}})}u_{\mathrm{s}} \\ \dot{x}_3 = \dot{z}_{\mathrm{u}} - \dot{q} = x_4 - \dot{q} \\ \dot{x}_4 = \ddot{z}_{\mathrm{u}} = \dfrac{kmm_{\mathrm{u}} + 2km_{\mathrm{i}}m_{\mathrm{u}} - 2km_i^2 - kmm_{\mathrm{i}}}{(m_{\mathrm{u}} - m_{\mathrm{i}})(mm_{\mathrm{u}} - mm_{\mathrm{i}} + m_{\mathrm{i}}m_{\mathrm{u}})}x_1 + \dfrac{cmm_{\mathrm{u}} + 2cm_{\mathrm{i}}m_{\mathrm{u}} - 2cm_{\mathrm{i}}^2 - cmm_{\mathrm{i}}}{(m_{\mathrm{u}} - m_{\mathrm{i}})(mm_{\mathrm{u}} - mm_{\mathrm{i}} + m_{\mathrm{i}}m_{\mathrm{u}})}x_2 \\ \qquad + \dfrac{k_{\mathrm{t}}m_{\mathrm{i}}^2 - k_{\mathrm{t}}mm_{\mathrm{u}} + k_{\mathrm{t}}mm_{\mathrm{i}} - k_{\mathrm{t}}m_{\mathrm{i}}m_{\mathrm{u}}}{(m_{\mathrm{u}} - m_{\mathrm{i}})(mm_{\mathrm{u}} - mm_{\mathrm{i}} + m_{\mathrm{i}}m_{\mathrm{u}})}x_3 + \dfrac{2cm_{\mathrm{i}}^2 - cm_{\mathrm{u}}}{(m_{\mathrm{u}} - m_{\mathrm{i}})(mm_{\mathrm{u}} - mm_{\mathrm{i}} + m_{\mathrm{i}}m_{\mathrm{u}})}x_4 \\ \qquad + \dfrac{3m_{\mathrm{i}}^2 + mm_{\mathrm{i}} - 2m_{\mathrm{i}}m_{\mathrm{u}} - mm_{\mathrm{u}}}{(m + m_{\mathrm{i}})(m_{\mathrm{u}} - m_{\mathrm{i}})^2}u_{\mathrm{s}} \end{cases} \tag{22}$$

$$\begin{aligned} y=\dot{x}_2 = & \frac{2km_\mathrm{i}-km_\mathrm{u}}{mm_\mathrm{u}-mm_\mathrm{i}+m_\mathrm{i}m_\mathrm{u}}x_1+\frac{2cm_\mathrm{i}-cm_\mathrm{u}}{mm_\mathrm{u}-mm_\mathrm{i}+m_\mathrm{i}m_\mathrm{u}}x_2-\frac{k_\mathrm{t}m_\mathrm{i}}{mm_\mathrm{u}-mm_\mathrm{i}+m_\mathrm{i}m_\mathrm{u}}x_3 \\ & -\frac{2cm_\mathrm{i}-cm_\mathrm{u}}{mm_\mathrm{u}-mm_\mathrm{i}+m_\mathrm{i}m_\mathrm{u}}x_4+\frac{m_\mathrm{u}-2m_\mathrm{i}}{(m+m_\mathrm{i})(m_\mathrm{u}-m_\mathrm{i})}u_\mathrm{s} \end{aligned} \tag{23}$$

where x_1 is the relative displacement between the sprung mass and wheel spring (i.e., $x_1 = z - z_\mathrm{u}$); x_2 is the vertical velocity of quarter car body (i.e., $x_2 = \dot{z}$); x_3 is the tire's elastic deformation (i.e., $x_3 = z_\mathrm{u} - q$); x_4 is the vertical velocity of wheel (i.e., $x_4 = \dot{z}_\mathrm{u}$).

The output vector $\mathbf{Y}$ is the response of the suspension system, i.e., $\mathbf{Y} = [\dot{x}_2]$, where $\dot{x}_2$ is the vertical acceleration of quarter car body. And the output vector can be written as:

The standard state equation of model in Eq. (1) can be written as:

$$\begin{cases} \dot{\mathbf{X}} = \mathbf{AX} + \mathbf{B}u_\mathrm{s} + \mathbf{H}\dot{q} \\ \mathbf{Y} = \mathbf{CX} + \mathbf{D}u_\mathrm{s} \end{cases} \tag{24}$$

where:

$$\mathbf{A} = \begin{bmatrix} 0 & 1 & 0 & -1 \\ \frac{2km_\mathrm{i}-km_\mathrm{u}}{mm_\mathrm{u}-mm_\mathrm{i}+m_\mathrm{i}m_\mathrm{u}} & \frac{2cm_\mathrm{i}-cm_\mathrm{u}}{mm_\mathrm{u}-mm_\mathrm{i}+m_\mathrm{i}m_\mathrm{u}} & -\frac{k_\mathrm{t}m_\mathrm{i}}{mm_\mathrm{u}-mm_\mathrm{i}+m_\mathrm{i}m_\mathrm{u}} & -\frac{2cm_\mathrm{i}-cm_\mathrm{u}}{mm_\mathrm{u}-mm_\mathrm{i}+m_\mathrm{i}m_\mathrm{u}} \\ 0 & 0 & 0 & 1 \\ \frac{kmm_\mathrm{u}+2km_\mathrm{i}m_\mathrm{u}-2km_\mathrm{i}^2-kmm_\mathrm{i}}{(m_\mathrm{u}-m_\mathrm{i})(mm_\mathrm{u}-mm_\mathrm{i}+m_\mathrm{i}m_\mathrm{u})} & \frac{cmm_\mathrm{u}+2cm_\mathrm{i}m_\mathrm{u}-2cm_\mathrm{i}^2-cmm_\mathrm{i}}{(m_\mathrm{u}-m_\mathrm{i})(mm_\mathrm{u}-mm_\mathrm{i}+m_\mathrm{i}m_\mathrm{u})} & \frac{k_\mathrm{t}m_\mathrm{i}^2-k_\mathrm{t}mm_\mathrm{u}+k_\mathrm{t}mm_\mathrm{i}-k_\mathrm{t}m_\mathrm{i}m_\mathrm{u}}{(m_\mathrm{u}-m_\mathrm{i})(mm_\mathrm{u}-mm_\mathrm{i}+m_\mathrm{i}m_\mathrm{u})} & \frac{2cm_\mathrm{i}^2-cm_\mathrm{u}}{(m_\mathrm{u}-m_\mathrm{i})(mm_\mathrm{u}-mm_\mathrm{i}+m_\mathrm{i}m_\mathrm{u})} \end{bmatrix},$$

$$\mathbf{B} = \begin{bmatrix} 0 \\ \frac{m_\mathrm{u}-2m_\mathrm{i}}{(m+m_\mathrm{i})(m_\mathrm{u}-m_\mathrm{i})} \\ 0 \\ \frac{3m_\mathrm{i}^2+mm_\mathrm{i}-2m_\mathrm{i}m_\mathrm{u}-mm_\mathrm{u}}{(m+m_\mathrm{i})(m_\mathrm{u}-m_\mathrm{i})^2} \end{bmatrix}, \quad \mathbf{D} = \begin{bmatrix} \frac{m_\mathrm{u}-2m_\mathrm{i}}{(m+m_\mathrm{i})(m_\mathrm{u}-m_\mathrm{i})} \end{bmatrix}, \quad \mathbf{H} = \begin{bmatrix} 0 \\ 0 \\ -1 \\ 0 \end{bmatrix},$$

$$\mathbf{C} = \begin{bmatrix} \frac{2km_\mathrm{i}-km_\mathrm{u}}{mm_\mathrm{u}-mm_\mathrm{i}+m_\mathrm{i}m_\mathrm{u}} & \frac{2cm_\mathrm{i}-cm_\mathrm{u}}{mm_\mathrm{u}-mm_\mathrm{i}+m_\mathrm{i}m_\mathrm{u}} & -\frac{k_\mathrm{t}m_\mathrm{i}}{mm_\mathrm{u}-mm_\mathrm{i}+m_\mathrm{i}m_\mathrm{u}} & -\frac{2cm_\mathrm{i}-cm_\mathrm{u}}{mm_\mathrm{u}-mm_\mathrm{i}+m_\mathrm{i}m_\mathrm{u}} \end{bmatrix}.$$

The design of the controller's performance is measured by output vector of Eq. (23), and the variable controllable force of u_s has limited power. So the performance index of suspension system can be written as:

$$J = \int_0^\infty \left(\mathbf{Y}^\mathrm{T}\mathbf{Y} + u_\mathrm{s}^T u_\mathrm{s}\right) dt \tag{25}$$

To find the optimum solution of u_s while J is the minimum value, the general solution of u_s can be described as:

$$u_\mathrm{s} = -\mathbf{KX} \tag{26}$$

where $\mathbf{KX}$ is a matrix of unknown. Substituting Eq. (26) to Eq. (25), the performance index can be rewritten as:

$$J = \int_0^\infty \mathbf{X}^\mathrm{T}\left(\mathbf{C}^\mathrm{T}\mathbf{C} - \mathbf{C}^\mathrm{T}\mathbf{DK} - \mathbf{K}^\mathrm{T}\mathbf{D}^\mathrm{T}\mathbf{C} + \mathbf{K}^\mathrm{T}\mathbf{D}^\mathrm{T}\mathbf{DK} + \mathbf{K}^\mathrm{T}\mathbf{K}\right)\mathbf{X}dt \tag{27}$$

If a matrix of $\mathbf{P}$ exists it satisfies (28):

$$\mathbf{X}^T\left(\mathbf{C}^\mathrm{T}\mathbf{C} - \mathbf{C}^\mathrm{T}\mathbf{DK} - \mathbf{K}^\mathrm{T}\mathbf{D}^\mathrm{T}\mathbf{C} + \mathbf{K}^\mathrm{T}\mathbf{D}^\mathrm{T}\mathbf{DK} + \mathbf{K}^\mathrm{T}\mathrm{K}\right)\mathbf{X} = -\frac{d}{dt}\left(\mathbf{X}^\mathrm{T}\mathbf{PX}\right) \tag{28}$$

Eq. (29) can be obtained on the basis of Eqs. (24) and (28), when the term of $\mathbf{A} - \mathbf{BK}$ is stable. The performance index is obtained as Eq. (30).

$$(\mathbf{A} - \mathbf{BK})^\mathrm{T}\mathbf{P} + \mathbf{P}(\mathbf{A} - \mathbf{BK}) = -\left(\mathbf{C}^\mathrm{T}\mathbf{C} - \mathbf{C}^\mathrm{T}\mathbf{DK} - \mathbf{K}^\mathrm{T}\mathbf{D}^\mathrm{T}\mathbf{C} + \mathbf{K}^\mathrm{T}\mathbf{D}^\mathrm{T}\mathbf{DK} + \mathbf{K}^\mathrm{T}\mathbf{K}\right) \tag{29}$$

$$J = \mathbf{X}^\mathrm{T}(0)\mathbf{PX}(0) \tag{30}$$

The matrix of **P** which is a function of **K** can be obtained from Eq. (29). J will be minimum on the condition of $\partial J/\partial \mathbf{K} = 0$. So **K** can be obtained, eventually.

5. EXPERIMENTAL SETUP AND RESULTS

Quarter-car regenerative semi-active suspension is organized as shown in Fig. 10.

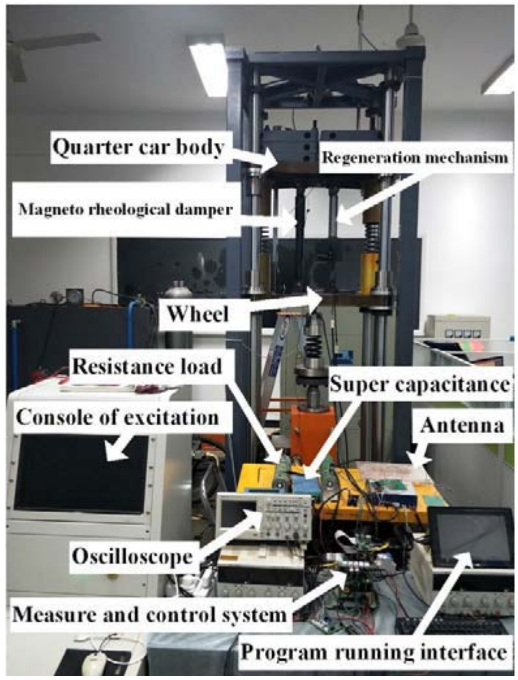

Figure 10. .Regenerative suspension prototype.

It is composed of a 2-DOF regenerative suspension system which recovers vibration energy from suspension system, a PT symmetric circuit which transmits power, a measure and control system, a console of excitation, and other accessories. The parameters of suspension system are tabulated in Table 2.

Table 2. Parameters of suspension system.

Parameter	Value
Quarter car body mass m	312.5 Kg
Wheel mass m_{u}	43.5 Kg
Inertial mass m_{i}	59 Kg
Physical spring coefficient k	2×10^4 N/m
Tire spring coefficient k_t	1.8×10^5 N/m
Physical permanent friction coefficient c	3639.8 N · s/m

Utilizing the parameters of suspension system, **K** of Eq. (26) is obtained as

$$\mathbf{K} = [\ 341.6 \quad 64.1 \quad -2813.5 \quad -73.8\ ] \tag{31}$$

So the optimum magneto rheological damping force can be rewritten as:

$$u_s = -341.6x_1 - 1604.6x_2 + 2813.5x_3 + 73.8x_4 \tag{32}$$

The regenerative suspension is actuated by a sine road profile having frequency of 1.27 Hz and amplitude of 15 mm. The voltages of source and receiver resonator are shown in Fig. 11. The result shows that the value of receiver is close to source. The loss is just 3.7%, so it is practical to recover energy all the time.

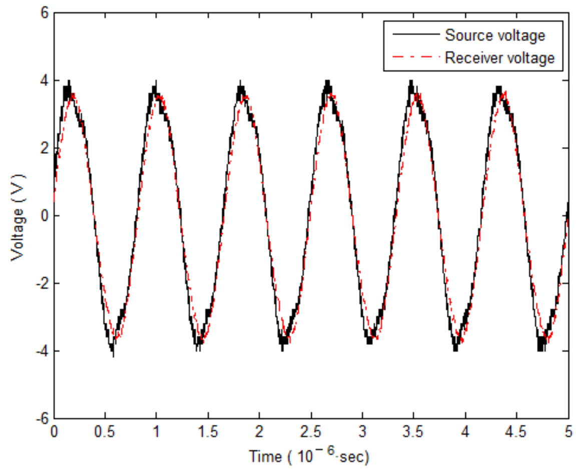

Figure 11. Voltage compare between source and receiver resonator.

Tests adopted to verify the design of PT symmetric circuit and control strategy are effective to suspension system's vibration controllability. We do tests under conditions of load resistance $R = 5\,\Omega$ without control strategy, PT symmetric circuit without control strategy, which is shown in Fig. 12. The vertical acceleration of quarter car body is more severe under PT symmetric circuit. Therefore, the electromagnetic damping force is useful to shock controllability of suspension system when no control strategy is used. The mean square root of vertical acceleration of quarter car body is $5.4\,\mathrm{m/s^2}$ when the electromagnetic damping force exists in the suspension. The frequency of walking is about 1.25 Hz in the vertical direction [22]. So the body does not feel uncomfortable if the vehicle vibrates vertically at this frequency. The most sensitive frequency of human body to vertical vibration is $4 \sim 12.5$ Hz, where $4 \sim 8$ Hz is the resonance frequency of human viscera, and the vibration of $8 \sim 12.5$ Hz has a great influence on the spine [23]. The maximum acceleration without control is higher than $0.315\,\mathrm{m/s^2}$, and the vertical vibration will make people feel uncomfortable within $8 \sim 12.5$ Hz, which is shown in Fig. 12(b). We do tests under conditions of skyhook control strategy and control strategy proposed in

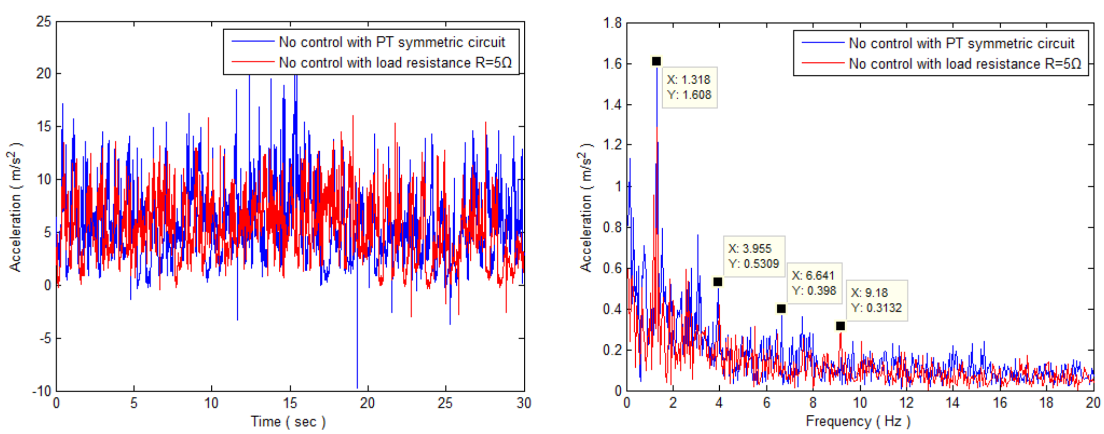

(a) Time domain signal (b) Frequency domain signal

Figure 12. Vertical acceleration compare of quarter car body without control on suspension system.

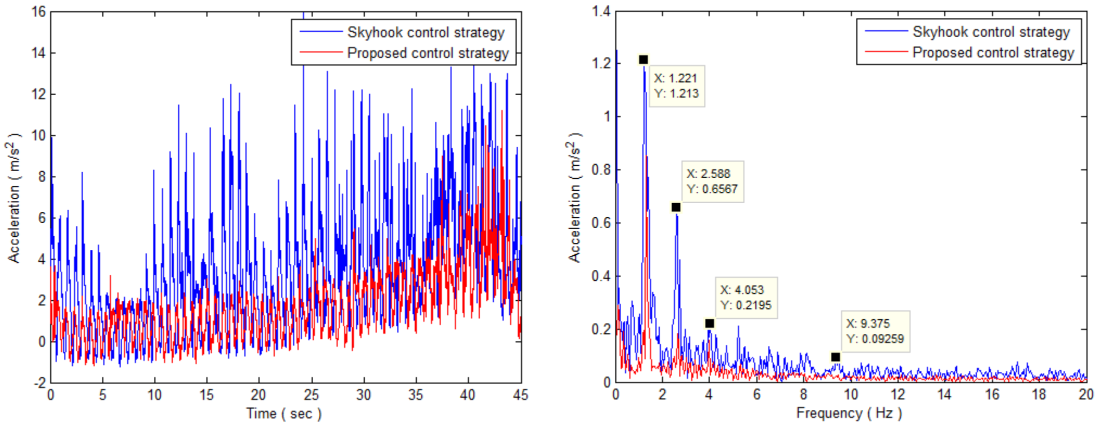

(a) Time domain signal (b) Frequency domain signal

Figure 13. Vertical acceleration compare of quarter car body with control on suspension system.

this paper with PT symmetric circuit, which is shown in Fig. 13. It shows that the proposed control strategy in this paper has better performance than skyhook control strategy, and the mean square root of vertical acceleration is only $1.1\,\mathrm{m/s^2}$. The maximum acceleration with control is lower than $0.315\,\mathrm{m/s^2}$, and the vertical vibration will make people feel comfortable within $8 \sim 12.5\,\mathrm{Hz}$. Especially, the acceleration is close to $0\,\mathrm{m/s^2}$ under proposed control strategy in this paper, which is shown in Fig. 13(b).

6. CONCLUSIONS

A semi-active suspension system prototype with a power regeneration mechanism has been studied in this paper. The designed suspension system is excited by a sine profile along with a control algorithm to reduce its inertial force. PT symmetric circuit is used to transmit power which is recovered from vibration energy. It could reduce electromagnetic damping force to the value of about 2N and recover energy of about 22 W when the relative speed of suspension system is $0.3\,\mathrm{m/s}$. Performance of the designed semi-active suspension system is verified in both load resistance and PT symmetric circuit modes, when the designed suspension system is under a sine road profile with frequency of 1.27 Hz and amplitude of 15 mm. According to the experimental results, the mean square root of vertical acceleration of the quarter car body is $1.1\,\mathrm{m/s^2}$, and the vertical acceleration is close to $0\,\mathrm{m/s^2}$ within $4 \sim 12.5\,\mathrm{Hz}$ when the designed suspension system is under the control strategy proposed in this paper and uses the PT symmetric circuit to transmit energy simultaneously.

REFERENCES

1. Amer, N. H., R. Ramli, H. M. Isa, W. N. L. Mahadi, and M. A. Z. Adidin, "A review of energy regeneration capabilities in controllable suspension for passenger's car," *EEST Part A: Energy Science and Research*, Vol. 30, No. 1, 143–145, 2012.
2. Zheng, X., F. Yu, and Y. Zhang, "A novel energy-regenerative active suspension for vehicles," *Journal of Shanghai Jiaotong University (Science)*, Vol. 02, No. 02, 184–188, 2008.
3. Montazeri-Gh, M. and M. Soleymani, "Investigation of the energy regeneration of active suspension system in hybrid electric vehicles," *IEEE Trans. Ind. Electron.*, Vol. 57, 918–925, 2010.
4. Martins, I., M. Esteves, F. Pina Da Silva, and P. Verdelho, "Electromagnetic hybrid active-passive vehicle suspension system," *IEEE 49th Veh. Tech. Conf.*, 2273–2277, 1999.
5. Paz, O. D., "Design and performance of electric shock absorber," MSc in Electrical Engineering Louisiana State University, 2004.

6. Okada, Y. and H. Harada, "Regenerative control of active vibration damper and suspension systems," *35th IEEE Decis. Control*, Vol. 4, 4715–4720, 1996.
7. Nakano K., Y. Suda, and S. Nakadai, " Self-powered active vibration control using a single electric actuator," *J. Sound Vib.*, Vol. 260, 213–235, 2003.
8. Lin, B. and X. Su, "Fault-tolerant controller design for active suspension system with proportional differential sliding mode observer," *International Journal of Control, Automation and Systems*, Vol. 17, No. 7, 1751–1761, 2019.
9. Majdoub, K. E., F. Giri, and F.-Z. Chaoui, "Adaptive backstepping control design for semi-active suspension of half-vehicle with magnetorheological damper," *IEEE/CAA Journal of Automatica Sinica*, Vol. 8, No. 03, 582–596, 2021.
10. Cho, Y., B. S. Song, and K. Yi, "A road-adaptive control law for semi-active suspensions," *KSME International Journal*, Vol. 13, No. 10, 667–676, 1999.
11. Peng, Z., "Research on vibration control and energy consumption of electromagnetic suspension system for tracked vehicle," Doctoral Dissertation, 1–5, College of machinery, Beijing China, December 2014.
12. Hu, P., "Research on the vibration control and energy-regenerative technologies of parallel composite electromagnetic suspension," Doctoral Dissertation, 102–105, College of machinery, Beijing China, December 2018.
13. Sharipov, G. M., D. S. Paraforos, and H. W. Griepentrog, "Implementation of a magnetorheological damper on a no-till seeding assembly for optimising seeding depth," *Computers & Electronics in Agriculture*, Vol. 150, 465–475, 2018.
14. Wang, X., "Research on the design and control of the energy-regenerative electromagnetic suspension system," Doctoral Dissertation, 43–45, College of machinery, Beijing China, December 2018.
15. Bender, C. M., D. C. Brody, and H. F. Jones, "Complex extension of quantum mechanics," *Phys. Rev. Lett.*, Vol. 89, 270401, 2002.
16. Feng, L., Z. J. Wong, R.-M. Ma, Y. Wang, and X. Zhang, "Single-mode laser by parity-time symmetry breaking," *Science*, Vol. 346, 972–975, 2014.
17. Sid, A., X. F. Yu, and S. H. Fan, "Robust wireless power transfer using a nonlinear parity-time-symmetric circuit," *Nature*, Vol. 546, 387–390, 2017.
18. Nakano, M., J. Yang, S. Sun, A. Totsuka, and A. Fukukita, "Development and damping properties of a seismic linear motion damper with MR fluid porous composite rotary brake," *Smart Materials and Structures*, Vol. 29, No. 11, 115043, 2020.
19. Zhang, H., H. Winner, and W. Li, "Comparison between skyhook and minimax control strategies for semi-active suspension system," *WASET*, 624–627, 2009.
20. Zhang, J., Z. Peng, and L. Zhang, "A review on energy-regenerative suspension systems for vehicles," *The World Congress on Engineering (WCE 2013)*, Vol. 3, 1889–1892, 2013.
21. Wang, X., J. Zhang, and Y. Liu, "An improved state feedback $\mathrm{H}\infty$control method within a finite frequency domain," *Journal of Vibration and Shock*, Vol. 38, No. 5, 135–140, 2019.
22. Chen, Z. and G. Liu, "Pedestrian-induced vibration theory and dynamic design of footbridges," *Engineering Mechanics*, Vol. 26, 148–152, 2009.
23. Standards, I., "Human response to vibration — Measuring instrumentation," BS EN ISO 8041-2005, 2005.